Observational Evidence of Reemergence in the Extratropical Southern Hemisphere

LAURA M. CIASTO* AND DAVID W. J. THOMPSON

Department of Atmospheric Science, Colorado State University, Fort Collins, Colorado

(Manuscript received 24 March 2008, in final form 19 September 2008)

ABSTRACT

Observations of subsurface temperatures are used to examine the winter-to-winter "reemergence" of sea surface temperature (SST) anomalies in the extratropical South Pacific Ocean. Reemergence is the mechanism through which SST anomalies formed in the late winter are sequestered beneath the relatively shallow summer mixed layer and then reentrained into the deepening mixed layer during the following autumn/winter. Although several studies have extensively examined reemergence in the Northern Hemisphere (NH), this is the first study to use observations of subsurface temperatures to document reemergence in the extratropical Southern Hemisphere (SH). The SH subsurface data reveal a pronounced reemergence signal in the western extratropical South Pacific. In this region, surface thermal anomalies formed during late SH winter are observed to persist below the summertime mixed layer and reemerge at the surface during the following early winter months. As such, SST anomalies formed during late winter are strongly correlated with SST anomalies during the following early winter but are not significantly correlated with SST anomalies during the intervening summer months. The results based on subsurface data are robust to small changes in the period of analysis and are qualitatively similar to existing evidence of reemergence in the NH. Analyses of independent SST data reveal that reemergence is widespread in the western extratropical South Pacific basin but is less discernible in SST anomalies over the eastern part of the basin.

1. Introduction

To first order, the persistence of extratropical sea surface temperature (SST) anomalies can be modeled as the damped thermodynamic response of the ocean mixed layer to white noise atmospheric forcing (Frankignoul and Hasselman 1977). Following the model developed in Frankignoul and Hasselman (1977), the large thermal inertia of the ocean mixed layer renders it sensitive to only the low-frequency part of the atmospheric forcing, and the SST field thus has a spectrum consistent with red noise. The result is that the *e*-folding time scale of the SST field can be as large as ~3–5 months despite the fact the forcing itself may have a decorrelation time scale of only a few days (Frankignoul and Hasselman 1977; Frankignoul and Reynolds 1983; Kushnir et al. 2002).

The persistence of extratropical SST anomalies can be enhanced beyond the ~3–5-month time scale suggested by the Frankignoul and Hasselman (1977) model by numerous factors, including the remote impact of the El Niño–Southern Oscillation (ENSO; Alexander et al. 2002), positive feedbacks between marine stratiform clouds and SST anomalies (e.g., Park et al. 2006), and the subduction and reentrainment of SST anomalies associated with the annual cycle of the mixed layer. The latter phenomenon was termed reemergence by Alexander and Deser (1995) and is examined here for the first time in the Southern Hemisphere (SH) using subsurface temperature observations.

Reemergence was first noted by Namias and Born (1970, 1974), who found that Northern Hemisphere (NH) extratropical SST anomalies tend to persist from one winter to the next but not through the intervening summer. They hypothesized that SST anomalies extending deep into the mixed layer are sequestered beneath the shoaling mixed layer during the spring and are thus insulated from the surface and atmospheric variability. When the mixed layer deepens in the subsequent autumn, the sequestered thermal anomalies are reentrained back into the ocean mixed layer. As a result, the

* Current affiliation: Climate Change Research Centre, University of New South Wales, Sydney, New South Wales, Australia.

Corresponding author address: Laura M. Ciasto, Climate Change Research Centre, University of New South Wales, Sydney, NSW 2052, Australia.
E-mail: l.ciasto@unsw.edu.au

DOI: 10.1175/2008JCLI2545.1

© 2009 American Meteorological Society

reemergence mechanism can increase the persistence of extratropical SST anomalies by more than a year (Deser et al. 2003).

Alexander and Deser (1995) provided observational evidence of the reemergence mechanism across the North Pacific and North Atlantic Oceans. Alexander et al. (1999) went on to explore the sensitivity of reemergence to the timing and location of the thermal anomaly and to the depth of the mixed layer across the extratropical North Pacific basin. Watanabe and Kimoto (2000) and de Coëtlogon and Frankignoul (2003) provided additional evidence of reemergence in the North Atlantic, and Timlin et al. (2002) revealed that reemergence is the leading mode of variability in extratropical North Atlantic subsurface temperature anomalies.

The reemergence of wintertime SST anomalies has been extensively documented in the extratropical NH but has received only cursory attention in the extratropical SH, presumably because of the lack of Southern Ocean subsurface ocean temperature observations. Hadfield (2000) noted that SSTs in the southeast Tasman Sea recur from spring to the following winter. Hanawa and Sugimoto (2004) noted that SST anomalies also recur in the central South Atlantic, the western Indian, and the western South Pacific Oceans. However, both of these studies relied primarily on satellite-derived SSTs; to our knowledge, no study has confirmed the existence of reemergence in the SH using subsurface temperature observations.

The goal of the present study is to use subsurface and surface temperature observations to explore the existence of reemergence in the extratropical South Pacific Ocean. Section 2 documents the data and methods used in this study, section 3 examines reemergence in the western South Pacific subsurface data, section 4 explores the spatial extent of the reemergence signal across the extratropical South Pacific basin using SST observations, and section 5 offers a summary of the results.

2. Data and methods

The upper ocean temperature profiles were obtained from the ''ENSEMBLES'' (EN3) dataset provided by the Met Office Hadley Centre (Ingleby and Huddleston 2007). A large fraction of the profiles in that dataset were originally from the World Ocean Database (WOD) 2005, a collection of more than 7 million ocean measurements gathered globally from ships, moored buoys, and drifting floats (Boyer et al. 2006). The WOD 2005 measurements are supplemented in the EN3 data by temperature profiles from the Global Temperature Salinity Profile Program as well as by temperature data collected from floating profilers provided by Argo. An automated control system is applied to the temperature profiles from the three sources, and duplicate profiles are discarded.

In the EN3 dataset, each individual month contains profiles of temperature for a given location (latitude/longitude) and depth (in meters). The quantity and positions of the profiles varies from month to month, and neither the locations of the profiles nor the depths at which temperatures are measured are regularly spaced. For example, January 1990 contains 9646 profiles of temperatures, but not all profiles are sampled at the same depths: the profile at 30°N, 22°W contains 141 temperature values at irregularly spaced depths from 0 to 2000 m, the profile at 61°S, 57°W contains 79 temperature values at irregularly spaced depths from 0 to 300 m, and so on.

Figure 1 shows the number of available vertical temperature profiles for the period 1990–2006 for the extratropical South Pacific. In actuality, the EN3 archive extends back to January 1950, but there are virtually no profile data in the SH prior to 1990. After 1990, temperature profiles are concentrated in the following three regions: 1) off the southeast coast of Australia, 2) to the north of New Zealand, and 3) to the south of Tasmania (Fig. 1). Of these regions, only the area north of New Zealand is marked by sufficiently weak currents to allow local reemergence to occur. In regions of strong currents, winter anomalies detrained from the ocean mixed layer are less likely to reemerge close to the source region (i.e., local reemergence) but could be advected away from the source region and reemerge farther downstream (de Coëtlogon and Frankignoul 2003). Therefore, the region east of Australia, which lies in a western boundary current exhibiting strong eddy activity (Nilsson and Cresswell 1981), and the region south of Tasmania, which lies in the Antarctic Circumpolar Current, are unlikely to exhibit local reemergence.

The subsurface data coverage is insufficient to examine the reemergence of advected thermal anomalies. We thus focus our analysis on local reemergence in the region to the north of New Zealand spanned by 30°–34°S and 170°E–180° (Fig. 1). The analysis region lies within an area of high data coverage but away from the influence of coastal processes. To convert monthly mean temperature profile data within the analysis region into monthly mean area-averaged anomaly temperature time series at discrete depth levels, the following steps are performed:

1) Because the levels at which temperatures were recorded vary between profiles, the temperatures from each profile were interpolated to nine discrete depth levels: 0, 10, 20, 30, 50, 75, 100, 125, and 150 m.

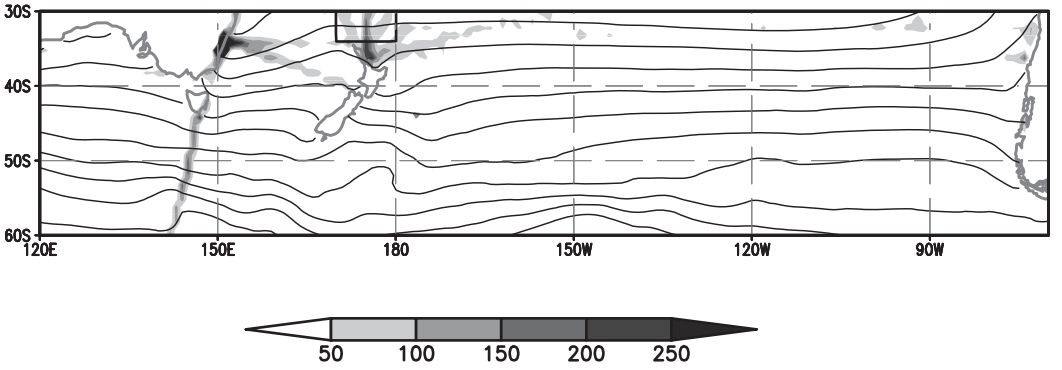

FIG. 1. Shading denotes the number of EN3 temperature profiles recorded within a 1° × 1° latitude–longitude box for the period 1990–2006. The solid contours denote the climatological annual mean SSTs. Contours are drawn at 2° intervals. The SST data are obtained from the NOAA OI SST dataset (see text for details).

2) Area-averaged temperatures were computed at all nine depth levels for two subsets of the analysis region: 30°–32°S, 170°E–180° and 32°–34°S, 170°E–180°. The subdivision was done to minimize the impact of missing data on our estimate of the seasonal cycle (e.g., the box-averaged seasonal cycle will be biased toward regions where there are the fewest missing data). In practice, the results were found to be stable to calculating temperature anomalies for subsets of the box or for the box as a whole.
3) The seasonal cycle was removed from the area-averaged temperatures found in step 2 by subtracting the long-term monthly mean from each month.
4) The temperature anomaly time series for the two subsets of the study region were averaged together to form monthly-mean time series at all nine depths. The resulting nine time series are indicative of temperature anomalies averaged over the region 30°–34°S, 170°E–180° at the depth levels given in step 1.

Monthly mean values of SSTs were obtained from the NOAA_OI_SST_V2 data (hereinafter referred to as the OI SST data) provided by the National Oceanic and Atmospheric Administration (NOAA) Office of Oceanic and Atmospheric Research/Earth System Research Laboratory in Boulder, Colorado, from their Internet site (http://www.cdc.noaa.gov/). The OI SST data are derived from a blended objective analysis of both in situ and satellite observations and were smoothed with a three-point binomial filter applied in both space and time (Reynolds et al. 2002). The OI SST data are available on a 1° × 1° latitude/longitude grid from 1981 to 2007, but the true resolution of the data is closer to 6° × 6° as discussed in O'Neill et al. (2003).

Mixed layer depth data were obtained from the Ocean Mixed Layer Depth Climatology dataset (http://www.lodyc.jussieu.fr/~cdblod/mld.html), as described in de Boyer Montégut et al. (2004). The data are available in monthly-mean format on a 2° × 2° mesh and were derived from over 4 million individual vertical profiles taken between 1941 and 2002, which are archived by the National Oceanographic Data Center and the World Ocean Circulation Experiment.

3. The reemergence signal in extratropical South Pacific subsurface temperature observations

The existence of reemergence depends on the amplitude of the seasonal cycle of the depth of the mixed layer: the winter mixed layer must be substantially deeper than the summer mixed layer (Timlin et al. 2002). Figure 2 shows the climatological mean mixed layer depths for the region 30°–34°S, 170°E–180°. The dashed line corresponds to the mixed layer depths derived from the Ocean Mixed Layer Depth Climatology dataset described in section 2. The solid line corresponds to the mixed layer depths calculated using the EN3 temperature data; the error bars denote the ±1 standard deviation range. The mixed layer depths are defined in both datasets as the depth at which the temperature differs from the temperature at 10 m by 0.2°C.

Both datasets reveal a strong seasonal cycle in the depth of the mixed layer. Relatively strong solar heating and weak surface winds during the SH summer drive mixed layer depths no deeper than ~25–30 m. Comparatively weak solar heating and strong surface winds drive mixed layer depths as deep as 100 m in SH winter. For the most part, the interannual standard deviation of the EN3-derived mixed layer depths is relatively small during the warm-season months (when the mixed layer is shallow). It is interesting that the standard deviation of the mixed layer is much larger during August–September than it is during April–May despite comparable mixed

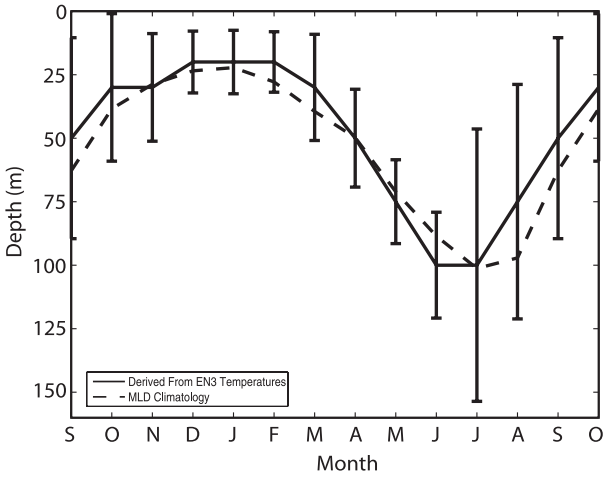

FIG. 2. Climatological mean mixed layer depth for the region 30°–34°S, 170°E–180° from EN3 temperature data (solid line) and the Ocean Mixed Layer Depth Climatology (dashed line). Error bars denote the ±1 std dev range. Mixed layer depth is defined as the depth at which the temperature differs from the temperature at 10 m by 0.2°C.

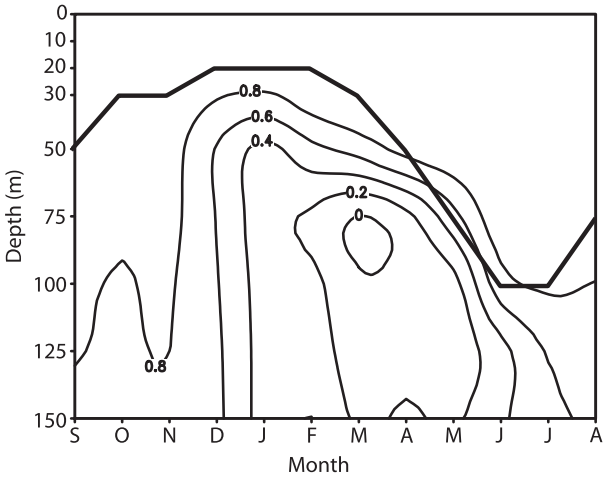

FIG. 3. Concurrent correlations between temperature anomalies at 0 m and temperature anomalies from 0 m down to 150 m for each month. For example, the correlation coefficient between temperature anomalies at 0 m and temperature anomalies at 50 m in January is 0.4. The thick black line corresponds to the climatological mean mixed layer depth derived from EN3 temperature data (see text for details).

layer depths at these times. One possible explanation for this feature is that the atmospheric circulation is more vigorous during the late winter season than it is during the autumn months.

Figure 3 shows the mean mixed layer depth from the EN3 data superposed on the pattern of concurrent correlations calculated for each month between temperature anomalies at the surface and temperature anomalies at all depths. For the most part, the seasonal cycle of the mixed layer depth in Fig. 1 is mirrored in the pattern of the correlations. In midsummer, the correlations between surface temperature anomalies and temperature anomalies at depth exceed 0.8 above ~30 m but decrease to less than 0.4 below 75 m. During winter, the 0.8 correlation contour drops to 100–125 m, which demonstrates that the layer of homogeneous temperatures extends considerably deeper at that time.

The most notable difference between the pattern of the correlations in Fig. 3 and the mixed layer depths from the EN3 climatological mean temperatures is found in the spring months (September–November), when the climatological mean mixed layer depth is only ~30–50 m but surface temperature anomalies are strongly correlated down to 125–150 m. A similar result was noted in Alexander and Deser (1995), who hypothesized that the depth of the correlations is determined by the scale of the vertical mixing during periods of enhanced springtime storm activity, whereas the depth of the mean mixed layer depth reflects an average over stormy and calm periods. An alternative explanation is that because the temperature anomalies at all levels exhibit substantial persistence the depth of the correlations during spring is determined by the depth of the vertical mixing during the previous winter.

To evaluate the reemergence signal in the subsurface data, we examine the temporal evolution of thermal anomalies in the upper ocean from one winter to the next. Studies that have investigated the reemergence signal in the NH have done so by examining lag correlations of thermal anomalies from one winter to the next. Here we adopt a similar method.

Figure 4 shows the lag correlations between temperature anomalies at 0 m in September and at 0–150 m for 0–13-month lags within the region 30°–34°S, 170°E–180°. In practice, qualitatively similar results are derived for correlations based on August and October temperature anomalies (not shown). The thick black line corresponds to the depths at which correlations with surface temperature anomalies exceed 0.8 (i.e., the 0.8 contour from Fig. 3), that is, the layer of homogenous temperature anomalies.

As also noted in Fig. 2, temperature anomalies in September are highly coupled throughout the top 125–150 m of the ocean. At the surface, the correlations decrease as a function of lag such that by December the surface temperature anomalies are not significantly correlated with surface temperature anomalies from the previous September (Fig. 3) but are correlated with temperature anomalies below the mixed layer (Fig. 2). The decay of the surface temperature anomalies from

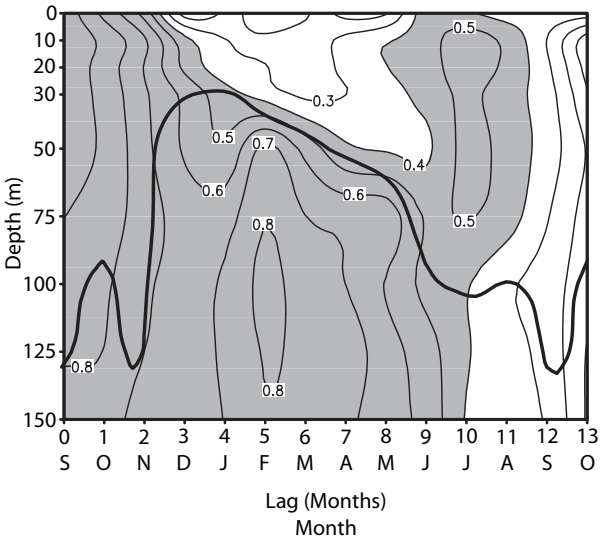

FIG. 4. Lag correlations between surface (0 m) temperature anomalies in September and temperature anomalies at standard depths for 0–13-month lags. For example, the correlation coefficient between September surface temperature anomalies and January temperature anomalies at 100 m is 0.7. Correlations that exceed 0.4 are shaded. The thick black line corresponds to the 0.8 contour line from Fig. 3.

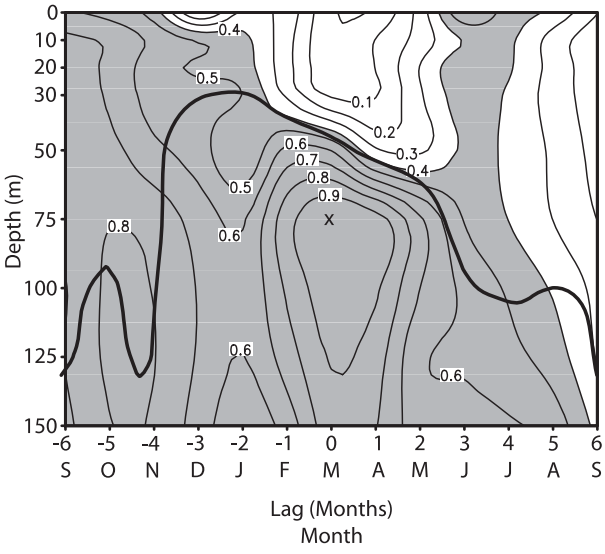

FIG. 5. Lead–lag correlations between temperature anomalies in March at 75 m (i.e., beneath the base of the summer mixed layer; marked by an X) and temperature anomalies at standard depths for the previous and following 6 months. For example, the correlation between March temperature anomalies at 75 m and temperature anomalies at 100 m in the previous October is 0.8. Correlations that exceed 0.4 are shaded. The thick black line corresponds to the 0.8 contour line from Fig. 3.

September to December is consistent with damping by anomalous heat fluxes at the ocean surface. In contrast, the temperature anomalies at depth in December are insulated from atmospheric influences. Hence, the temperature anomalies below about 50 m remain significantly correlated throughout the summer season with the subsurface and surface anomalies formed during the previous September.

The deepening mixed layer throughout the autumn allows the thermal anomalies sequestered within the seasonal thermocline to be reentrained into the mixed layer. Thus, in June and July, temperature anomalies throughout the mixed layer are impacted by the entrainment process and become significantly correlated with surface temperature anomalies formed during the previous September. By July, the mixed layer encompasses the entire top 100 m of the ocean and the SST anomalies that were formed 11 months earlier (and stored beneath the summertime mixed layer) are finally damped to the overlying atmosphere.

The structure of the reemergence signal is also clearly evident if the temperature anomalies below the summer mixed layer are used as a basis for the correlations. Figure 5 shows that March temperature anomalies at 75 m are significantly correlated with temperature anomalies at all depths during the previous September–November as well as the following June–July. The results in Fig. 5 reveal that the temperature anomalies beneath the summertime mixed layer originate in part from within the mixed layer during the previous winter and are decoupled from contemporaneous temperature anomalies at the surface.

The results in Figs. 4 and 5 are broadly consistent with the results of subsurface data in the North Atlantic and Pacific Oceans (Alexander and Deser 1995; Alexander et al. 1999; Timlin et al. 2002). As noted earlier, the pattern of reemergence evident in Fig. 4 is robust to changes in the start month of the correlations (e.g., if the analysis is based on August or October). Furthermore, qualitatively similar results to Fig. 5 are obtained for correlations based on temperature anomalies at a range of months and depths during the summer season.

4. The surface signature of reemergence across the extratropical South Pacific

In this section, monthly OI SST anomalies are used to independently assess the reemergence mechanism in the extratropical southern Pacific Ocean. We first use the OI SST data to more closely examine the robustness of reemergence in the region 30°–34°S, 170°E–180°. Figure 6 shows the lag correlations between area-averaged SST anomalies based on three different start months (August, September, and October). Note that the *x* axis in Fig. 6

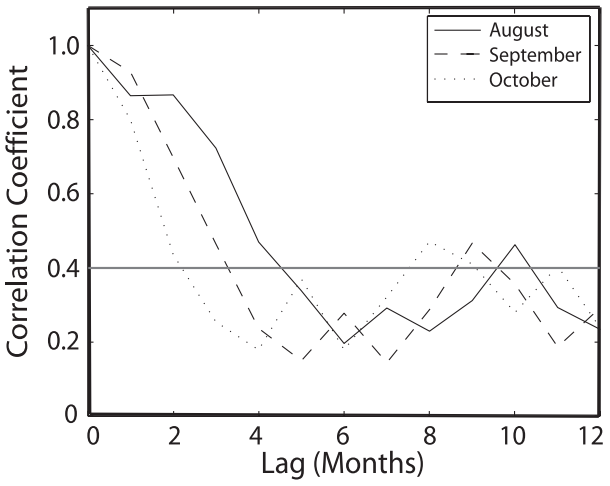

FIG. 6. Lag correlations of OI SST anomalies averaged over the region 30°–34°S, 170°E–180° based on a starting month of August (solid line), September (dashed line), and October (dotted line). For example, at lag 6, the solid line corresponds to a correlation between August and February SST anomalies of ~0.2. The horizontal gray line corresponds to the 95% confidence level.

is a function of lag relative to the basis month for the correlations. For example, lag 4 corresponds to correlations between August and December SST anomalies (solid line), September and January SST anomalies (dashed line), and October and February SST anomalies (dotted line).

The results in Fig. 6 demonstrate that the reemergence signal in the region 30°–34°S, 170°E–180° is robust to small changes in the start month, consistent with the results found using the subsurface data. Whether the SST anomalies are formed in August, September, or October, they are only weakly correlated with February SST anomalies but are significantly correlated with June SST anomalies when mixed layer depths are deepest (see Fig. 2). In all three cases, the correlations between wintertime SST anomalies and June SST anomalies are statistically significant at the 95% confidence level and are also broadly consistent with the subsurface results in Figs. 4 and 5.

We now use the OI SST data to examine the signal of reemergence across the entire extratropical South Pacific basin. Figure 7 shows the lag correlations between SST anomalies in September and SST anomalies in November, January, March, May, July, and the following September at all grid points in the extratropical South Pacific Ocean. The left panel corresponds to correlations calculated for the period 1990–2006, the same period used to analyze the subsurface EN3 temperature anomalies in the previous section. The right panel corresponds to the correlations calculated for the period 1982–2007, the full OI SST record. Correlations exceeding 0.4 and 0.35 are significant at the 95% confidence level for the left and right panels, respectively.

Both the left and right panels in Fig. 7 exhibit a statistically significant reemergence signal in the western part of the extratropical South Pacific basin but no reemergence signal over the eastern part of the basin. In the western extratropical South Pacific, September SST anomalies are weakly correlated with SST anomalies in the spring/summer (January–March) but are strongly correlated with SST anomalies in the following winter (May–September). The amplitude of the correlations tend be slightly stronger for the period 1990–2006 than for the full record, but the structures are qualitatively similar for both periods. Neither period of analysis suggests that reemergence is occurring over the eastern extratropical South Pacific.

The restriction of reemergence in the extratropical South Pacific SST field to longitudes west of 150°W is consistent with the results in Hanawa and Sugimoto (2004), who provided a global survey of recurring lag correlations in the SST field. It is unclear why reemergence is indiscernible over the eastern part of the extratropical South Pacific because the seasonal cycle in the ocean mixed layer exhibits a large seasonal cycle there (not shown). One possible explanation is that SST variability associated with ENSO preferentially obscures the reemergence signal in the eastern part of the extratropical South Pacific. However, we view this explanation as unlikely because qualitatively similar results to those shown in Fig. 7 are obtained when ENSO is linearly regressed from the SST time series at each grid point (not shown). Another possible explanation is that there is insufficient sampling in the eastern extratropical South Pacific to detect reemergence in that region. The Advanced Very High Resolution Radiometer satellite used in part to derive the OI SSTs does not ''see'' through cloud decks (e.g., O'Neill et al. 2003), which are widespread in the eastern extratropical South Pacific. Additionally, in situ SST observations are much more prevalent in the western part of the basin than in the eastern part (e.g., Reynolds et al. 2002). Unfortunately, there are insufficient subsurface temperature observations in the eastern extratropical South Pacific to assess whether reemergence is also absent in subsurface data.

5. Summary and discussion

Previous studies have examined the reemergence of extratropical wintertime SST anomalies in the North Atlantic and North Pacific (Alexander and Deser 1995; Bhatt et al. 1998; Alexander et al. 1999, 2001; Timlin et al. 2002). Reemergence has been noted in the South

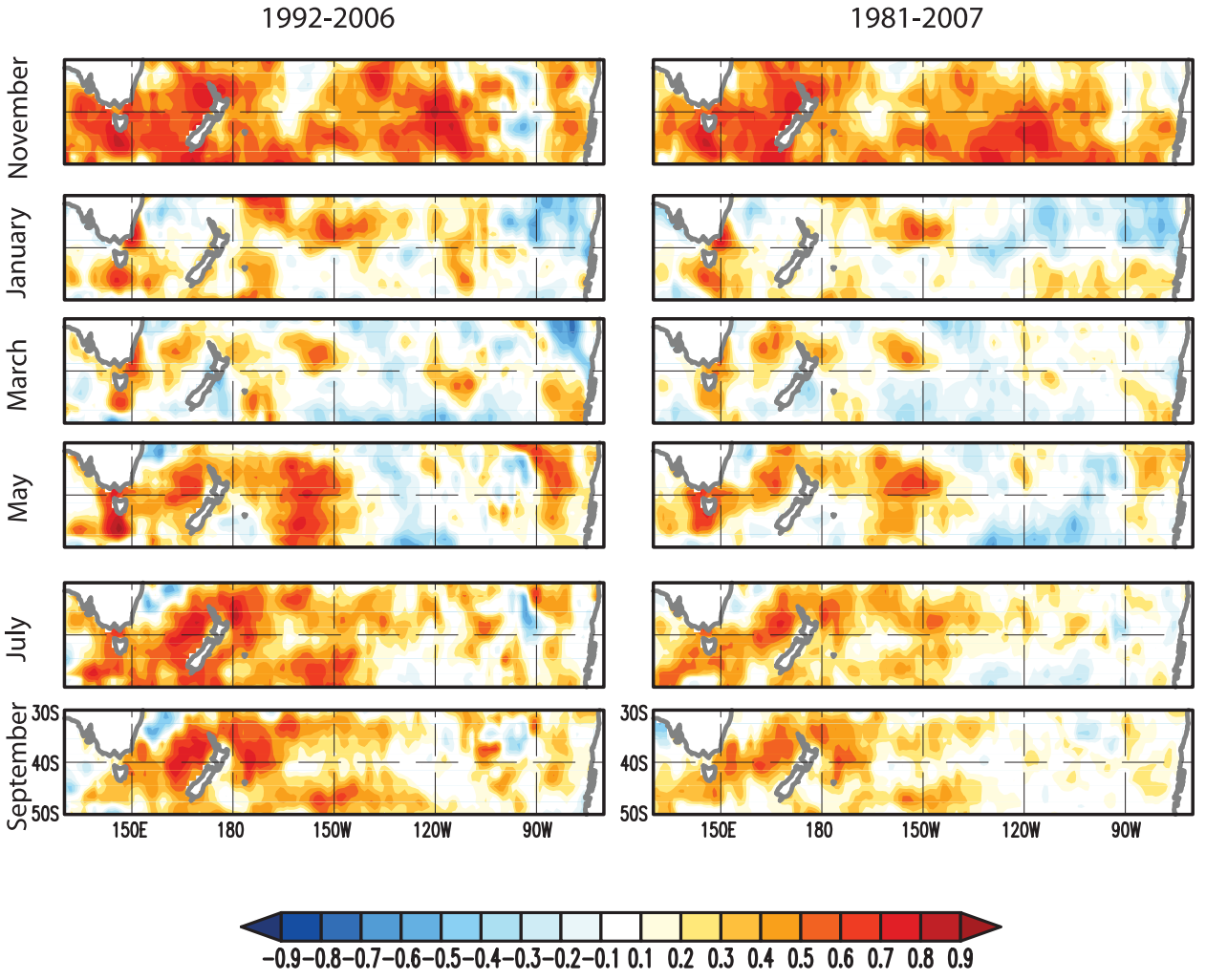

FIG. 7. Correlations between September SST anomalies and SST anomalies for (top) November, (second from top) January, (third from top) March, (third from bottom) May, (second from bottom) July, and (bottom) the following September for the periods (left) 1990–2006 and (right) 1982–2007.

Pacific, Indian, and South Atlantic Oceans in a global survey of recurring lag correlations in the SST field (Hanawa and Sugimoto 2004) and in National Centers for Environmental Prediction SST data in the southeast Tasman Sea (Hadfield 2000). To our knowledge, this is the first study to explicitly prove the existence of reemergence in the SH using observations of subsurface temperatures.

Our analysis of subsurface data is limited by the scarcity of observations in the extratropical SH ocean basins and is thus restricted to the region 30°–34°S, 170°E–180°, which lies in the western part of the extratropical South Pacific Ocean to the north of New Zealand. Consistent with the reemergence mechanism, the analyses show that SST anomalies formed in the late winter/early spring are significantly related to SST anomalies observed in the following autumn/winter but are unrelated to SST anomalies in the intervening summer. The analyses also reveal that temperature anomalies beneath the mixed layer in the summer are strongly correlated with temperature anomalies within the mixed layer during the previous and following winters but are weakly correlated with temperature anomalies within the summer mixed layer. Thus, consistent with the reemergence mechanism, the results suggest that wintertime SST anomalies tend to persist beneath the summer mixed layer and are reentrained in the subsequent autumn/winter. The reemergence of SH SST anomalies explains ~21% of the year-to-year variance in the June SST field over the western South Pacific. The results based on the SH subsurface temperature data are generally consistent with the behavior of reemergence observed in the NH (Alexander and Deser 1995; Alexander et al. 1999; Timlin et al. 2002).

Sea surface temperature data were used to independently evaluate the spatial scale of the winter-to-winter recurrence of SST anomalies across the extratropical South Pacific basin. The results reveal that the reemergence mechanism is evident throughout the western part of the South Pacific basin, where late winter SST anomalies are weakly correlated with SST anomalies in the spring/summer but significantly correlated with SST anomalies in the following autumn/winter. The results also reveal that the reemergence signal is less discernible in the eastern part of the extratropical South Pacific basin.

The results of the current study demonstrate that the reemergence of SST anomalies in the extratropical South Pacific yields predictability in anomalous SSTs out to ~8–10 months, which is longer than the known predictability associated with most other physical phenomena. It is unclear if the reemerging SST anomalies impact the extratropical atmospheric circulation, but, if they do, reemergence may prove to be important for seasonal forecasting.

Acknowledgments. The authors thank the three anonymous reviewers for comments and suggestions, which improved the manuscript. We also thank Drs. Michael A. Alexander and Clara Deser for helpful discussions of the results. This research was supported by the NSF under Grants ATM-0613082 and ATM-0132190.

REFERENCES

Alexander, M. A., and C. Deser, 1995: A mechanism for the recurrence of wintertime midlatitude SST anomalies. *J. Phys. Oceanogr.,* **25,** 122–137.

——, ——, and M. S. Timlin, 1999: The reemergence of SST anomalies in the North Pacific Ocean. *J. Climate,* **12,** 2419–2433.

——, M. S. Timlin, and J. D. Scott, 2001: Winter-to-winter recurrence of sea surface temperature, salinity, and mixed layer depth anomalies. *Prog. Oceanogr.,* **49,** 41–61.

——, I. Bladé, M. Newman, J. R. Lanzante, N.-C. Lau, and J. D. Scott, 2002: The atmospheric bridge: The influence of ENSO teleconnections on air–sea interaction over the global oceans. *J. Climate,* **15,** 2205–2231.

Bhatt, U. S., M. A. Alexander, D. S. Battisti, D. D. Houghton, and L. M. Keller, 1998: Atmosphere–ocean interaction in the North Atlantic: Near-surface climate variability. *J. Climate,* **11,** 1615–1632.

Boyer, T. P., and Coauthors, 2006: *World Ocean Database 2005*. NOAA Atlas NESDIS 60, S. Levitus, Ed., 190 pp.

de Boyer Montégut, C., G. Madec, A. S. Fischer, A. Lazar, and D. Idicone, 2004: Mixed layer depth over the global ocean: An examination of profile data and a profile-based climatology. *J. Geophys. Res.,* **109,** C12003, doi:10.1029/2004JC002378.

de Coëtlogon, G., and C. Frankignoul, 2003: The persistence of winter sea surface temperatures in the North Atlantic. *J. Climate,* **16,** 1364–1377.

Deser, C., M. A. Alexander, and M. S. Timlin, 2003: Understanding the persistence of sea surface temperature anomalies in midlatitudes. *J. Climate,* **16,** 57–72.

Frankignoul, C., and K. Hasselman, 1977: Stochastic climate models. Part II: Application to sea–surface temperature variability and thermocline variability. *Tellus,* **29,** 289–305.

——, and R. W. Reynolds, 1983: Testing a dynamical model for mid-latitude sea surface temperature anomalies. *J. Phys. Oceanogr.,* **13,** 1131–1145.

Hadfield, M. G., 2000: Atmospheric effects on upper-ocean temperature in the southeast Tasman Sea. *J. Phys. Oceanogr.,* **30,** 3239–3248.

Hanawa, K., and S. Sugimoto, 2004: 'Reemergence' areas of winter sea surface temperature anomalies in the world's oceans. *Geophys. Res. Lett.,* **31,** L10303, doi:10.1029/2004GL019904.

Ingleby, B., and M. Huddleston, 2007: Quality control of ocean temperature and salinity profiles—Historical and real-time data. *J. Mar. Syst.,* **65,** 158–175.

Kushnir, Y., W. A. Robinson, I. Bladé, N. M. J. Hall, S. Peng, and R. Sutton, 2002: Atmospheric GCM response to extratropical SST anomalies: Synthesis and evaluation. *J. Climate,* **15,** 2233–2256.

Namias, J., and R. M. Born, 1970: Temporal coherence in North Pacific sea-surface temperature patterns. *J. Geophys. Res.,* **75,** 5952–5955.

——, and ——, 1974: Further studies of temporal coherence in North Pacific sea surface temperatures. *J. Geophys. Res.,* **79,** 797–798.

Nilsson, C. S., and G. R. Cresswell, 1981: The formation and evolution of East Australian Current warm-core eddies. *Prog. Oceanogr.,* **9,** 133–183.

O'Neill, L. W., D. B. Chelton, and S. K. Esbensen, 2003: Observations of SST-induced perturbations of the wind stress field over the Southern Ocean on seasonal timescales. *J. Climate,* **16,** 2340–2354.

Park, S., M. A. Alexander, and C. Deser, 2006: The impact of cloud radiative feedback, remote ENSO forcing, and entrainment on the persistence of North Pacific sea surface temperature anomalies. *J. Climate,* **19,** 6243–6261.

Reynolds, R. W., N. Rayner, T. M. Smith, D. C. Stokes, and W. Wang, 2002: An improved in situ and satellite SST analysis for climate. *J. Climate,* **15,** 1609–1625.

Timlin, M. S., M. A. Alexander, and C. Deser, 2002: On the reemergence of North Atlantic SST anomalies. *J. Climate,* **15,** 2707–2712.

Watanabe, M., and M. Kimoto, 2000: On the persistence of decadal SST anomalies in the North Atlantic. *J. Climate,* **13,** 3017–3028.